

Optimization-Based Analysis of Modulation Instability in Resonant Cavities

Guy Klemens, *Member, IEEE*, and Yeshiahu Fainman, *Fellow, IEEE*

Abstract—We present an optimization-based method for the analysis of modulation instability effects in a resonant cavity. This method allows for varying levels of approximation in the solution and for the inclusion of effects such as loss or gain, if significant. The method is then demonstrated with examples showing the effects of the cavity modes on the gain curves.

Index Terms—Nonlinear optics, nonlinear wave propagation, optical frequency conversion, optical resonators.

I. INTRODUCTION

WAVE packets propagating through a nonlinear, dispersive medium can, under the right conditions, lose energy to sidebands. This effect, called modulation instability (MI), has been theoretically analyzed [1] and experimentally observed [2], [3] for light propagating through fibers. MI occurs when the intensity-dependent nonlinear effects compensate for the phase-mismatch caused by material dispersion. Analytical derivations of MI assume freely propagating waves in an infinite medium, and are not applicable in the case of a resonant cavity. In such a cavity, an unlimited number of reflected beams interact, greatly complicating the solution. The case of ring cavities, in which pulses of waves propagate around a loop of optical fiber, without multiple interfering beams, has been examined [4], [5] using the approximate analytical formulation of MI in an unbounded medium with periodicity imposed. We present an analysis method that can efficiently simulate MI effects in a resonant cavity, including wave interference in both directions. The proposed method is generally applicable, allowing for the inclusion of any number of nonlinear effects and frequency products, or for multiple coupled resonant cavities to be simulated.

The procedure we use assumes the steady-state has been reached, and tests input and output field values to find a set that satisfies all boundary conditions and nonlinear equations. This is similar in principle to the harmonic balance method used in nonlinear circuit analysis [6]. Balance is reached when the field values at the left of the cavity, when applied to the boundary conditions and the nonlinear equations, produce the field values on the right of the cavity, and similarly for propagation from right to left in the cavity. If the set of field values does not balance, then an error term can be defined and

the set adjusted to lower the error. The energy transfer between the waves in MI is found from coupled nonlinear differential equations [7]. A similar method has been applied to optical nonlinear wavelength conversion [8], such as second-harmonic generation, in a cavity. That work offers more information on optimization-based simulation of nonlinear optics.

The following section explains the use of this method for simulating MI in a one-dimensional resonant structure. This includes stating the equations involved and showing how varying levels of approximation can be used in the calculations. The subsequent section demonstrates the use of this technique with numerical examples.

II. ANALYSIS METHOD

A. Coupled Nonlinear Differential Equations

The starting point of the analysis is to represent Maxwell's equations with the second-order nonlinearity in the form of coupled differential equations [9]. For a plane wave traveling along the z -axis, the wave equation for the electric field is

$$\frac{\partial^2 E}{\partial z^2} = \varepsilon_0 \frac{\partial^2}{\partial t^2} \left[\varepsilon_r E + \chi^{(2)} EE + \chi^{(3)} EEE + \dots \right] \quad (1)$$

where ε_0 is the permittivity of free space, ε_r is the (frequency-dependent) relative permittivity, and $\chi^{(m)}$ are the nonlinear coefficients. Loss is modeled by including an imaginary component in the relative permittivity. We consider here a wave at frequency ω_0 , which we call the pump beam, and two equally spaced sideband frequencies of $\omega_+ = \omega_0 + \Omega$ and $\omega_- = \omega_0 - \Omega$. Accordingly, the electric field in (1) is expanded as $E = E_0 e^{-i\omega_0 t} + E_+ e^{-i\omega_+ t} + E_- e^{-i\omega_- t} + c.c.$, with c.c. denoting complex conjugate. A full range of frequencies are produced in the propagation described by (1), including harmonics and intermodulation products. As many of these frequency terms can be included in the following analysis as are needed for accuracy. If the assumption is made that frequency components other than the three listed are limited by phase-mismatch that is not compensated by nonlinear effects, then (1) becomes three coupled differential equations

$$\frac{d^2 E_0}{dz^2} = -\frac{\omega_0^2}{c^2} \left[n_0^2 E_0 + \chi^{(3)} (3|E_0|^2 + 6|E_+|^2 + 6|E_-|^2) E_0 + 6\chi^{(3)} E_+ E_- E_0^* \right] \quad (2)$$

$$\frac{d^2 E_+}{dz^2} = -\frac{\omega_+^2}{c^2} \left[n_+^2 E_+ + \chi^{(3)} (6|E_0|^2 + 3|E_+|^2 + 6|E_-|^2) E_+ + 3\chi^{(3)} E_0 E_0 E_-^* \right] \quad (3)$$

Manuscript received April 8, 2007; revised September 12, 2007. This work was supported in part by the Defense Advanced Research Projects Agency (DARPA) and by the National Science Foundation (NSF).

The authors are with the Department of Electrical and Computer Engineering, University of California, San Diego, La Jolla, CA 92093 USA.

Digital Object Identifier 10.1109/LPT.2007.913240

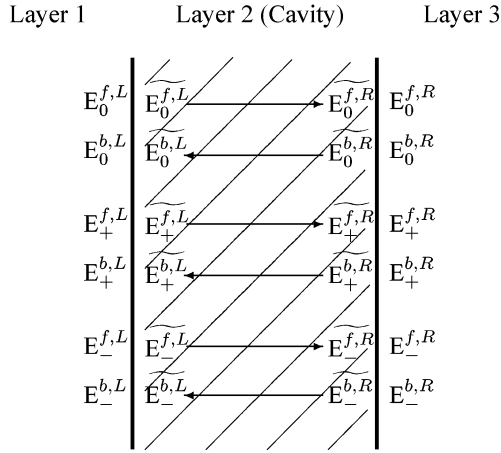


Fig. 1. Steady-state variable assignment for a single cavity. Fields are propagated across the cavity using coupled differential equations and the results compared to the expected values.

$$\frac{d^2 E_-}{dz^2} = -\frac{\omega_-^2}{c^2} \left[n_-^2 E_- + \chi^{(3)} (6|E_0|^2 + 6|E_+|^2 + 3|E_-|^2) E_- + 3\chi^{(3)} E_0 E_0 E_+^* \right]. \quad (4)$$

If the field intensity, dispersion, and nonlinear coefficient are at certain values, solving these equations numerically will show MI for a propagation length. The MI gain sidebands are characterized by solving the coupled equations repeatedly for values of Ω varying from a small value to several terahertz. A small initial value of A_+ and A_- is needed for all cases to show MI output.

B. Optimization-Based Solution Method

The steady-state case to be solved is outlined in Fig. 1. There are 12 complex variables made up of the forward and backward traveling waves at both sides of the cavity at the three frequencies. We will assume that there are no waves incident from the right side, so $E_0^{b,R}$, $E_+^{b,R}$, and $E_-^{b,R}$ are all held constant at zero. Also, the waves entering from the left side, $E_0^{f,L}$, $E_+^{f,L}$, $E_-^{f,L}$, are set to known values. This leaves six complex unknowns, representing the reflected and transmitted waves, to be solved. Multiple coupled cavities can be represented similarly, with each interface adding six complex unknowns. Equations (2)–(4) describe the propagation and energy transfer between the three steady-state waves across each cavity in one direction. The waves propagating in the opposite direction are also modeled with these three equations using different starting values. The two sets of three equations are largely decoupled by the phase-mismatch of counterpropagating waves. The total fields, however, are needed for the squared amplitude terms, so the forward and backward sets of equations are not completely decoupled.

Values are assumed for the six complex variables and then the calculations are performed to find if the case is balanced. First the external variables are translated inside the cavity using the reflection and transmission coefficients. The internal field values are represented in Fig. 1 with tildes. Then variables $E_0^{f,L}$, $E_+^{f,L}$, and $E_-^{f,L}$ are used as starting values in the coupled differential

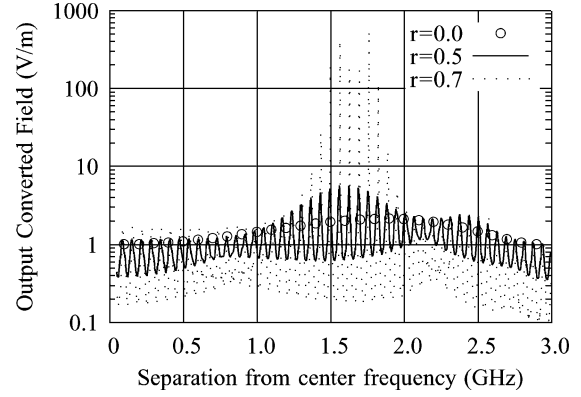


Fig. 2. Calculated MI output of an example cavity, for different end-mirror reflection coefficients. The sideband initial values were 1 W/m^2 . Values of index dispersion and nonlinear constant were used to clearly show the effects of the resonant cavity.

equations. The resulting values are compared with $\widetilde{E}_0^{f,R}$, $\widetilde{E}_+^{f,R}$, and $\widetilde{E}_-^{f,R}$ for a match. Similarly, the backward traveling waves at the right interface are propagated across the cavity and the results compared with the values at the left interface. The six comparisons will show no differences for a balanced case, meaning that the set of values is consistent with all of the boundary conditions and the nonlinear equations. If the comparisons do not yield a match, then an error term can be defined as the sum of the squares of the differences. Optimization methods can then be used to re-assign values to the complex variables to lower the error. We used a conjugate-gradient algorithm to perform the optimization, as was done in [8]. Once calculation shows that the error term associated with a set of values is near zero, then those values can be used as the solution.

III. EXAMPLES

A. Small Cavity Examples

To clearly show the effects of a resonant cavity on MI, it is instructive first to construct a case that clearly shows cavity modes. We set the material dispersion and nonlinear coefficient so that MI can be visible over a propagation length of only 10 cm, with a pump wavelength of $1.319 \mu\text{m}$. The nonlinear coefficient was set to $\chi^{(3)} = 5 \times 10^{-14} \text{ m}^2/\text{V}^2$. The full dispersion equations can be used, although the critical parameter for MI is the group velocity dispersion which is described by the second derivative of the index, set to $d^2n/d\omega^2 = -10^{-29} \text{ s}^2$ for this example. The effect of adding mirrors to the ends of the propagation length are shown in Fig. 2. The peak of MI gain occurs at the same sideband frequency, although the magnitude is changed and the resonances of the cavity are clearly visible. Increasing the reflection coefficient of the mirrors further increases the MI output.

B. Semiconductor Cavity

We consider here the calculation of MI in resonant cavities with relatively high nonlinear coefficients, such as semiconductors (on the order of $10^{-14} \text{ cm}^2/\text{V}^2$, compared to $10^{-16} \text{ cm}^2/\text{V}^2$ for glass). The pump beam used for the example had a wavelength of $1.319 \mu\text{m}$ and amplitude $5 \times 10^7 \text{ W/m}^2$,

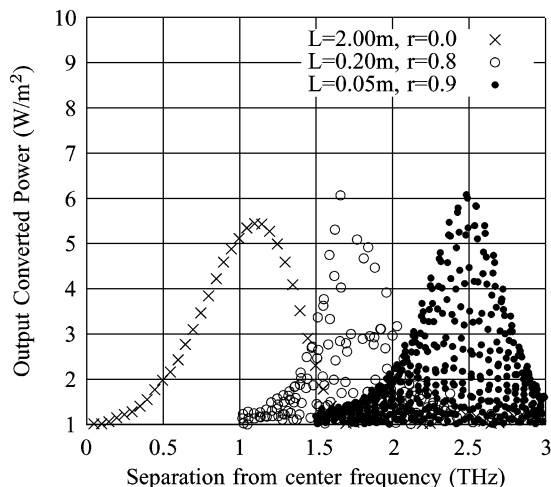


Fig. 3. Calculated MI output of a sample cavity of different lengths and end-mirror reflectivity. The high-finesse cavities have narrow and closely spaced peaks, which are only approximately indicated in this figure.

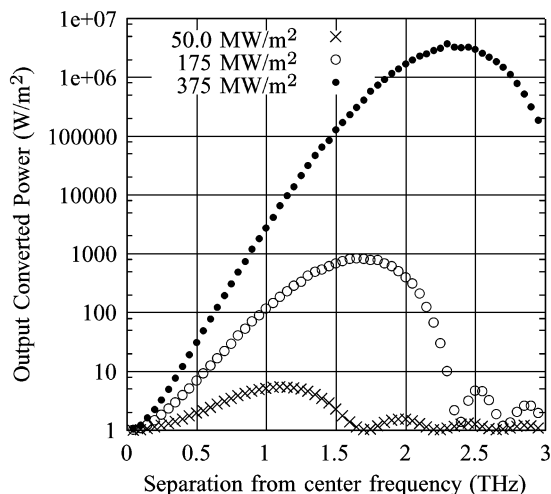


Fig. 4. Calculated MI output of a sample propagation length with no end mirrors. The pump beam is increased in each data set to correspond with the finesse of the resonant cavities in Fig. 3.

the negative group velocity dispersion regime is assumed. Fig. 3 shows the results of several optimization-based calculation runs. The open propagation length without the cavity is a theoretical 2-m length of semiconductor, and shows MI gain. The subsequent data points in the figure are for cavity lengths of 0.2 and 0.05 m, with the mirror reflectivity increased to compensate for the shorter propagation lengths. As the reflectivity of the end mirrors increases, the frequency of maximum MI gain shifts upward.

We can approximately predict the frequency shift of the MI gain maximum in a resonant cavity by using the cavity finesse. The cavity finesse, which is calculated from the mirror reflection coefficient r by $F = \pi r / (1 - r^2)$, is approximately equal to the number of interfering beams in the cavity. The pump beam

propagating in each direction is, therefore, increased by a factor of $0.5 F$. The reflection coefficients of Fig. 3 correspond to factors of 3.5 and 7.5, which have been applied to the pump beam amplitude for a propagation length with no end mirrors in Fig. 4. The frequencies of peak MI gain occur at the same locations as for the resonant cavities of Fig. 3. The amplitudes of output MI are different, however, due to the different propagation lengths used to generate the two figures. This shift in the peak MI frequency is also consistent with the standard derivation of MI [1], which predicts a frequency offset proportional to the electric field magnitude (square root of the intensity).

IV. CONCLUSION

By testing trial solutions of the field values and converging on a set of values that satisfies all boundary conditions and propagation equations, we can efficiently solve for the effects of MI in a resonant cavity. The complications involved in a transient analysis or an analytic solution are avoided. For MI in a cavity, the complications can become excessive since each case contains at least six interacting waves, along with all of their reflections. Furthermore, an optimization-based method offers flexibility in the level of approximation made and the effects, such as loss, that can be included. Applying this new solution method to resonant cavities, we are able to show that the resonance increases the MI output over what would appear in a similar cavity length with no end mirrors. Furthermore, in a high-finesse cavity, the pump beam can be increased in magnitude enough to shift the frequency of the MI gain maximum higher. MI could, therefore, occur in a relatively short propagation length if there are end-mirrors with sufficient reflectivity and the cavity is in resonance.

REFERENCES

- [1] A. Hasegawa and W. F. Brinkman, "Tunable coherent IR and FIR sources utilizing modulational instability," *IEEE J. Quantum Electron.*, vol. 16, no. 7, pp. 694–697, Jul. 1980.
- [2] K. Tai, A. Hasegawa, and A. Tomita, "Observation of modulational instability in optical fibers," *Phys. Rev. Lett.*, vol. 56, no. 2, pp. 135–138, Jan. 13, 1986.
- [3] M. J. Potasek and G. P. Agrawal, "Self-amplitude-modulation of optical pulses in nonlinear dispersive fibers," *Phys. Rev. A*, vol. 36, no. 8, pp. 3862–3867, 1987.
- [4] M. Nakazawa, K. Suzuki, and H. A. Haus, "The modulational instability laser—Part I: Experiment," *IEEE J. Quantum Electron.*, vol. 25, no. 9, pp. 2036–2044, Sep. 1989.
- [5] M. Haelterman, S. Trillo, and S. Wabnitz, "Additive-modulation-instability ring laser in the normal dispersion regime of a fiber," *Opt. Lett.*, vol. 17, no. 10, pp. 745–747, 1992.
- [6] S. El-Rabaie, V. F. Fusco, and C. Stewart, "Harmonic balance evaluation of nonlinear microwave circuits—A tutorial approach," *IEEE Trans. Educ.*, vol. 31, no. 3, pp. 181–192, Aug. 1988.
- [7] W. Huang and J. Hong, "A coupled-mode analysis of modulation instability in optical fibers," *J. Lightw. Technol.*, vol. 10, no. 2, pp. 156–162, Feb. 1992.
- [8] G. Klemens and Y. Fainman, "Optimization-based calculation of optical nonlinear processes in a micro-resonator," *Opt. Express*, vol. 14, pp. 9864–9872, 2006.
- [9] J. A. Armstrong, N. Bloembergen, J. Ducuing, and P. S. Pershan, "Interactions between light waves in a nonlinear dielectric," *Phys. Rev.*, vol. 127, no. 6, pp. 1918–1939, Sep. 15, 1962.